

Dirty Weyl semimetals: Stability, phase transition, and quantum criticality

Soumya Bera,¹ Jay D. Sau,² and Bitan Roy²

¹Max-Planck-Institut für Physik Komplexer Systeme, 01187 Dresden, Germany

²Condensed Matter Theory Center, Department of Physics, University of Maryland, College Park, Maryland 20742, USA

(Received 3 August 2015; revised manuscript received 25 April 2016; published 17 May 2016)

We study the stability of three-dimensional incompressible Weyl semimetals in the presence of random quenched charge impurities. Combining numerical analysis and scaling theory, we show that, in the presence of sufficiently weak randomness, (i) the Weyl semimetal remains stable, while (ii) the double-Weyl semimetal gives rise to compressible diffusive metal where the mean density of states at zero energy is finite. At stronger disorder, the Weyl semimetal undergoes a quantum phase transition and enter into a metallic phase. The mean density of states at zero energy serves as the order parameter and displays single-parameter scaling across such a disorder driven quantum phase transition. We numerically determine various exponents at the critical point, which appear to be insensitive to the number of Weyl pairs. We also extract the extent of the quantum critical regime in disordered Weyl semimetals and the phase diagram of dirty double-Weyl semimetals at finite energies.

DOI: 10.1103/PhysRevB.93.201302

Introduction. Over the span of the past few years the horizon of topological phases of matter has been extended beyond the gapped states [1,2] and now includes various nodal (gapless) systems as well [3,4]. Three-dimensional Weyl semimetals (WSMs) are the prime example of such noninsulating systems, which are constituted by so-called Weyl nodes that act as the source (monopole) and sink (antimonopoles) for *Berry flux* in the reciprocal space, thus always appearing in pairs [5]. As the hallmark signature of a topologically nontrivial phase, WSM accommodates gapless (chiral) surface states that can give rise to peculiar electromagnetic responses, such as anomalous Hall and chiral-magnetic effects [6]. While gapped topological phases are expected to be robust against sufficiently weak randomness, the stability of their gapless counterpart against disorder demands careful investigation and constitutes the central theme of this Rapid Communication.

Recently, we have witnessed the discovery of WSMs in a number of noncentrosymmetric and magnetic semiconductors [7–16]. Various other proposals for WSMs, for example, include antiferromagnetically [17] or spin-ice [18] ordered pyrochlore iridates, multilayer configurations of topological and regular insulators [19,20], and magnetically doped topological insulators [21]. The monopole charge of Weyl nodes in these systems is ± 1 . Nevertheless, HgCr_2Se_4 [22] and SrSi_2 [23] are expected to host Weyl nodes with a monopole charge ± 2 , dubbed as the double WSM. The topological invariant and enclosed Berry flux in double WSMs are twice that in a WSM, and consequently the one-dimensional chiral surface states in the former system possess a twofold degeneracy. Although electromagnetic responses in Weyl materials are reasonably well understood [6], the stability of incompressible topological semimetals in the presence of quenched randomness is yet to be explored and settled. This is the quest that has recently culminated in a surge of analytical [24–34] and numerical [35–44] works and we pursue it here for WSM and double WSM, using numerical and analytical methods.

We address the stability of these two systems against randomly quenched charge impurities by analyzing the mean density of states (MDOS) at zero energy, where nondegenerate valence and conduction bands touch each other. Our central results are as follows: (i) For sufficiently weak disorder,

while WSMs remain stable, the double WSM undergoes a *BCS-like weak coupling instability* toward the formation of a compressible diffusive metal (CDM), where the MDOS at zero energy is finite (see Fig. 1). (ii) WSMs undergo a disorder driven quantum phase transition (QPT), beyond which the system becomes a CDM. (iii) Across the WSM-CDM transition, MDOS display single-parameter scaling and within our numerical accuracy the critical exponents at such an *itinerant* quantum critical point (QCP) appear to be insensitive to the number of Weyl pairs (N_W) (see Table I).

Model. A paradigmatic two-band toy model,

$$H_W = \sum_{\mathbf{k}} \Psi_{\mathbf{k}}^{\dagger} [N_1(\mathbf{k})\sigma_1 + N_2(\mathbf{k})\sigma_2 + N_3(\mathbf{k})\sigma_3] \Psi_{\mathbf{k}}, \quad (1)$$

can describe different members of the Weyl family, where σ are standard Pauli matrices. Fermionic annihilation operators $c_{s,\mathbf{k}}$ with spin projections $s = \uparrow, \downarrow$ and wave vector \mathbf{k} constitute the two-component spinor $\Psi_{\mathbf{k}}^{\top} = (c_{\uparrow,\mathbf{k}}, c_{\downarrow,\mathbf{k}})$. A WSM is found upon choosing $N_j(\mathbf{k}) = t \sin(k_j a)$ for $j = 1, 2$, $N_3(\mathbf{k}) = N_3^1(\mathbf{k}) + N_3^2(\mathbf{k})$, where $2N_3^1(\mathbf{k}) = t \cos(k_3 a)$ and a is the lattice spacing. In this model, the number of Weyl pairs (N_W) can be tuned efficiently by the *Wilson mass* $N_3^2(\mathbf{k}) = t' [b - \cos(k_1 a) - \cos(k_2 a)]$. A double WSM can be constructed by taking $N_1(\mathbf{k}) = t_1 [\sin(k_1 a) - \sin(k_2 a)]$, $N_2(\mathbf{k}) = t_1 \cos(k_1 a) \cos(k_2 a)$, and $N_3^2(\mathbf{k}) = t' [2 - \sin(k_3 a) -$

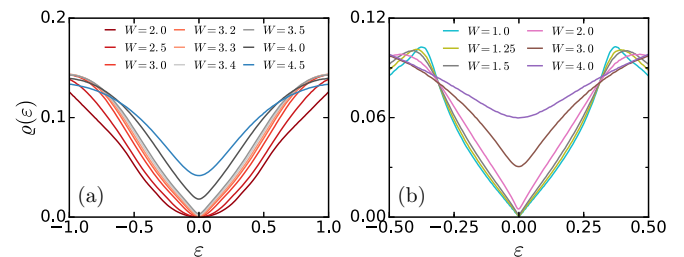


FIG. 1. MDOS in (a) WSM ($N_W = 1$) and (b) double WSM. WSM remains stable up to $W_c = 3.3 \pm 0.1$, beyond which the mean DOS at $\varepsilon = 0$, $\rho(0)$ is finite, and the system becomes a CDM. The double WSM visibly turns into a CDM for weak enough disorder, $W \gtrsim 1.0$.

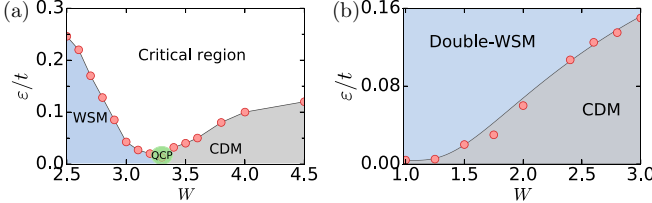


FIG. 2. Finite energy phase diagram of a dirty (a) WSM ($N_w = 1$) and (b) double WSM, for $L = 220$.

$\sin(k_y a)$], while keeping $N_3^1(\mathbf{k})$ unaltered. We implement these tight-binding models on a cubic lattice with a periodic boundary in each direction [45].

Disorder. The quintessential properties of dirty Weyl systems can be established from their effective low energy theory in the close vicinity of the Weyl points. The low energy Hamiltonians for WSM and double WSM are

$$H_1 = \Psi_\tau^\dagger [-i\tau(\sigma_1\partial_1 + \sigma_2\partial_2 + \tau\sigma_3\partial_3) + V(\mathbf{r})]\Psi_\tau, \quad (2)$$

$$H_2 = \Psi_\tau^\dagger \left[\sigma_1 \frac{\partial_2^2 - \partial_1^2}{2m} - \sigma_2 \frac{2\partial_1\partial_2}{2m} - i\tau\sigma_3\partial_z + V(\mathbf{r}) \right] \Psi_\tau, \quad (3)$$

respectively, where $v \sim ta$, $m^{-1} \sim t_1 a^2$, $\tau = \pm$ represent left and right chiral sectors, respectively, and we set $t = t' = t_1 = 1 = a$. The effect of random impurities is captured by $V(\mathbf{r})$, distributed uniformly and independently within $[-\frac{W}{2}, \frac{W}{2}]$, and the MDOS is numerically evaluated using the kernel polynomial method [36,45,46].

To gain insights into the role of disorder in these systems, we can perform disorder averaging, assuming a Gaussian white noise distribution with zero mean, i.e., $\langle \langle V(\mathbf{r})V(\mathbf{r}') \rangle \rangle = \Delta\delta^3(\mathbf{r} - \mathbf{r}')$, and arrive at the replicated Euclidean action

$$\begin{aligned} \bar{S}_n = & \int d^3x dt (\Psi_a^\dagger [\partial_t + \tilde{H}_n] \Psi_a)_{(x,t)} \\ & - \frac{\Delta}{2} \int d^3x dt dt' (\Psi_a^\dagger \Psi_a)_{(x,t)} (\Psi_b^\dagger \Psi_b)_{(x,t')}, \end{aligned} \quad (4)$$

where a, b are replica indices and \tilde{H}_n corresponds to the Hamiltonian from Eqs. (2) and (3) in the clean limit. The scale invariance of physical observables (v and m) dictates the following space-time (imaginary) scaling ansatz: $(x, y) \rightarrow e^{l/n}(x, y)$, $z \rightarrow e^l z$, and $t \rightarrow e^l t$, accompanied by the rescaling of fermionic field $\Psi \rightarrow e^{-(\frac{l}{n} + \frac{1}{2})l} \Psi$, where $l \sim \log \frac{L}{a}$ is the scaling parameter. The scaling dimension of disorder coupling is $[\Delta] = 1 - \frac{2}{n}$. Hence, sufficiently weak disorder is an *irrelevant* (since $[\Delta] = -1$) and a *marginally relevant* (since $[\Delta] = 0$) perturbation in WSM and double WSM, respectively [45]. Therefore, WSM (double WSM) is expected to be stable (unstable) in the presence of sufficiently weak randomness.

Notice that $[\Delta] \equiv 2z - d$ [45], where d is dimensionality of the system and z is the dynamic critical exponent, together governing the scaling of mean DOS $\varrho(\varepsilon) \sim |\varepsilon|^{d/z-1}$. Therefore, with $z = 1$ and $\frac{3}{2}$, $\varrho(\varepsilon) \sim |\varepsilon|^2$ and $|\varepsilon|$, respectively, for WSM and double WSM, in agreement with our numerical findings (see Fig. 1).

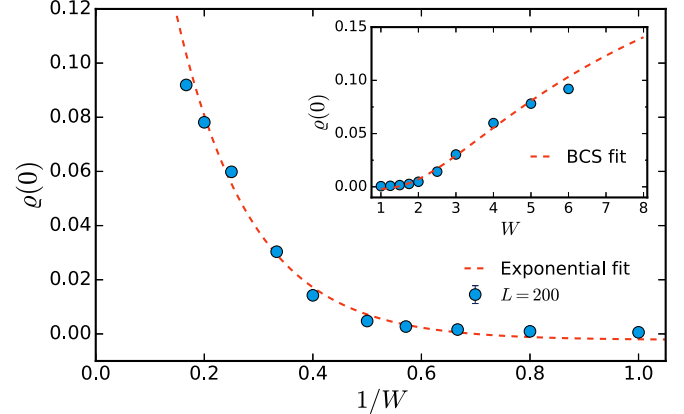


FIG. 3. MDOS at zero energy $\varrho(0)$ in double WSM as a function of $1/W$. Inset: Scaling of $\varrho(0)$ with W .

Stability. WSM evidently remains stable for weak disorder ($W \lesssim 3.3$) and MDOS at zero energy $\varrho(0) = 0$, in agreement with our scaling theory [see Fig. 1(a)]. However, for strong disorder, WSM appears to undergo a QPT and enters into the CDM phase, where $\varrho(0)$ becomes finite. A finite energy phase diagram of a dirty WSM is shown in Fig. 2(a). This observation is in qualitative agreement with various field theoretic [24–29] and numerical analyses for three-dimensional Dirac [35,36,38,40] and Weyl [39,41,42] semimetals. We will discuss the nature of such a QPT in a moment.

The scaling analysis suggests a BCS-like instability of double WSM toward the formation of CDM for infinitesimal randomness, and a phase diagram of this system is shown in Fig. 2(b). By contrast, available data of $\varrho(0)$ for double WSM in a finite system suggest a putative threshold value of disorder ($W_{th} \approx 1$), only beyond which $\varrho(0)$ is visibly finite [Fig. 1(b)]. To examine whether the observed finite $\varrho(0)$ is a consequence of a $W = 0^+$ instability, we compare $\varrho(0)$ vs $1/W$ (see Fig. 3). It is evident that larger systems are required to pin the exponential onset of $\varrho(0)$ for sufficiently weak W , as $W_{th} \sim 1/\log(L)$. Still, $\varrho(0)$ depicts an overall good agreement with an exponential decrease with $1/W$. In addition, $\varrho(0)$ fits very well with the celebrated BCS scaling form $\varrho(0) \sim \exp(-\lambda/W)$, with the nonuniversal parameter $\lambda = 7.2 \pm 0.8$ (see the inset of Fig. 3). Instability of double WSM against weak enough disorder is, however, insensitive to the nature of the disorder, and a similar outcome holds for magnetic disorders [45]. But $\varrho(0)$ starts to deviate from BCS scaling for $W > 5.0$ and falls below the exponential line. Such behavior can be attributed to the well-known Anderson transition of a three-dimensional metal, across which MDOS does not display critical behavior, but decreases monotonically [38]. We anticipate that for $W > 5.0$ the double WSM falls within the basin of attraction of the metal-Anderson insulator critical point. However, due to a *logarithmic* onset of a metallic phase in dirty double WSM, for sufficiently weak disorder and/or small system size, quasiparticle excitations can retain their ballistic nature over a large energy scale [see Fig. 2(b)].

Criticality. Now we investigate the scaling of MDOS across a disorder driven QPT in WSM. The total number of states $\mathcal{N}(\varepsilon, L)$ below the energy ε in a system of linear size L is proportional to L^d , and in general is a function of two

TABLE I. Comparison of critical disorder for WSM-CDM QPT (W_c), dynamic critical exponent (z), and correlation length exponent (ν) extracted from the scaling of MDOS (see text) for WSM with $N_W = 1, 2, 4$ [45]. Quantities in parentheses denote the fitting error. Near the WSM-CDM QPT at strong disorder all nodes get coupled, and with increasing backscattering channels or N_W , W_c gradually decreases.

N_W	W_c	z	ν_M	ν_W	ν_L
1	$3.3(0.1)$	$1.42(0.05)$	$0.97(0.1)$	$0.72(0.2)$	$0.95(0.1)$
2	$2.5(0.1)$	$1.38(0.05)$	$1.1(0.15)$	$0.72(0.2)$	$1.1(0.15)$
4	$2.2(0.1)$	$1.49(0.05)$	$0.86(0.06)$	$0.8(0.15)$	$0.9(0.1)$

dimensionless variables L/ξ and $\varepsilon/\varepsilon_0$. While the correlation length diverges as $\xi \sim \delta^{-\nu}$, the corresponding energy scale vanishes according to $\varepsilon_0 \sim \delta^{\nu z}$, as one approaches the QCP ($\delta \rightarrow 0$), where $\delta = (W - W_c)/W_c$ measures the deviation from the QCP (W_c) and ν is the correlation length exponent [47,48]. Consequently,

$$\mathcal{N}(\varepsilon, L) = (L/\xi)^d \mathcal{G}(\varepsilon \delta^{-\nu z}, L^{1/\nu} \delta), \quad (5)$$

where \mathcal{G} is an unknown scaling function. From the definition of MDOS, $\varrho(\varepsilon, L) = L^{-d} d\mathcal{N}(\varepsilon, L)/d\varepsilon$, we then arrive at the following scaling ansatz,

$$\varrho(\varepsilon, L) = \delta^{v(d-z)} \mathcal{F}(|\varepsilon| \delta^{-\nu z}, L^{1/\nu} \delta), \quad (6)$$

after accounting the particle-hole symmetry, $\varrho(\varepsilon, L) = \varrho(-\varepsilon, L)$, where \mathcal{F} is also an unknown, but a universal scaling function. Below we demonstrate the scaling analysis of MDOS in WSM with $N_W = 1$ and the results for $N_W = 1, 2$, and 4 are summarized in Table I [45].

First, we consider a sufficiently large system ($L = 220$), so that the finite size effects are negligible and L dependence in Eq. (6) can be ignored. From the scaling of MDOS at zero energy $\varrho(0)$ with disorder we estimate critical disorder for the WSM-CDM QPT $W_c = 3.3 \pm 0.1$ [Fig. 4(a)]. At the QCP ($\delta = 0$), the δ dependence of $\varrho(\delta)$ must cancel out, demanding $F(x) \sim x^{\frac{d}{z}-1}$, and therefore $\varrho(\delta) \sim |\delta|^{\frac{d}{z}-1}$. From Fig. 4(b) we obtain $z = 1.42 \pm 0.05$.

In the metallic phase, the MDOS at zero energy $\varrho(0)$ is finite and serves as the order parameter. In this regime $\varrho(0) \sim \delta^{(d-z)\nu}$ and one can identify $(d-z)\nu$ as the order parameter exponent (β). However, such a power law dependence of $\varrho(0)$ is valid when $\xi \ll L$. Therefore, we fit $\varrho(0)$ as $\delta^{(d-z)\nu}$ for $\delta \geq 0.06$, and obtain $\nu_M = 0.97 \pm 0.1$, where ν_M is the correlation length exponent extracted from the metallic phase [see Fig. 4(c)].

In WSM, the mean DOS scales as $\varrho(\varepsilon) \sim c(\delta)^{-1} |\varepsilon|^{d-1}$, so that we recover $\varrho(\varepsilon) \sim |\varepsilon|^2$ for $d = 3$, where $c(\delta) \sim \delta^{(z-1)d\nu_W}$ and ν_W is the correlation length exponent extracted from the WSM phase. However, it should be noted that for $W < W_c$, the mean DOS displays a smooth crossover from $|\varepsilon|^2$ (for small ε) to $|\varepsilon|$ (for large ε) dependence. Therefore, estimation of ν_W depends crucially on the range over which we attempt to fit $\varrho(\varepsilon) \sim |\varepsilon|^2$, and the accuracy of ν_W can be questioned. Nevertheless, by fitting the coefficient of $|\varepsilon|^2$ with $c(\delta)^{-1}$, we obtain $\nu_W = 0.72 \pm 0.2$ [see Fig. 4(d)].

Data collapse. We now demonstrate that $\varrho(\varepsilon)$ displays a single-parameter scaling across the WSM-CDM QPT. First,

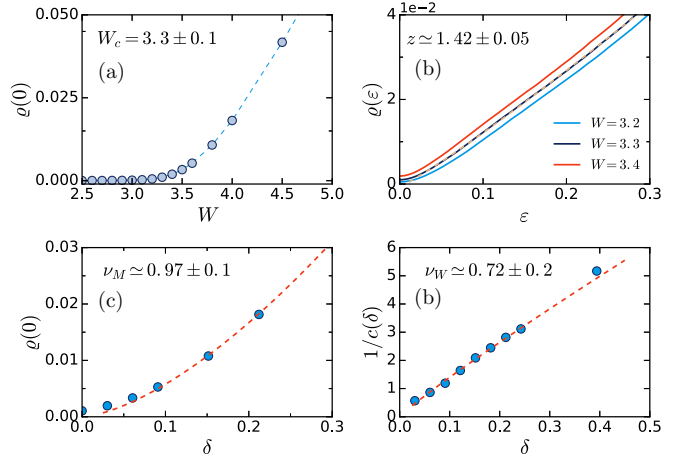


FIG. 4. (a) MDOS at zero energy $\varrho(0)$ vs disorder; (b) MDOS $\varrho(\varepsilon)$ vs ε for $W = 3.2, 3.3, 3.4$; (c) $\varrho(0)$ vs δ , where $\delta = (W - W_c)/W_c$; (d) $c(\delta)^{-1}$ vs δ , with $c(\delta) = \delta^{(z-1)d\nu}$, for WSM with $N_W = 1$, assuming $W_c = 3.3$ [45].

we compare $\varrho(\varepsilon)\delta^{-(d-z)\nu}$ vs $|\varepsilon|\delta^{-z\nu}$ for $L = 220$. Neglecting the high energy part of the spectrum ($|\varepsilon| > 0.5$) outside the Weyl cones and the extremely small energy ($|\varepsilon| < 10^{-2}$) where numerical accuracy is small, we find that all data from Fig. 1(a) collapse onto two separate branches, associated with the CDM and WSM phases [see Fig. 5(a)].

Next, we delve into the finite size data collapse for MDOS at $\varepsilon = 0$ and estimate ν independently. Setting $\varepsilon = 0$ in Eq. (6), we obtain $\varrho(0, L) = L^{z-d} \mathcal{F}(0, \delta L^{1/\nu})$. An excellent data collapse is achieved by comparing $\varrho(L, 0)L^{d-z}$ with $\delta L^{1/\nu}$ for several systems with $80 < L < 180$, $W_c = 3.3$, and $z = 1.42$ [see Fig. 5(b)]. The correlation length exponent extracted from the best quality data collapse is $\nu_L = 0.95 \pm 0.1$. Thus, $\varrho(0)$ displays a single-parameter scaling and serves as an bona fide order parameter across the WSM-CDM QPT.

Critical regime. The crossover from the quadratic (at small energy) to the linear (for higher energies) scaling of $\varrho(\varepsilon)$ allows us to estimate the crossover boundary between the WSM and critical regime at finite energy when $W < W_c$. For sufficiently weak disorder, $\varrho(\varepsilon) \sim |\varepsilon|^2$ over a wide range of energy. As the randomness is gradually increased (but still $W < W_c$), more and more degrees of freedom need to be integrated out (in the spirit of the renormalization group) to wash out the effect of disorder from the system. Consequently, the energy window over which $\varrho(\varepsilon) \sim |\varepsilon|^2$ gets reduced and the region where $\varrho(\varepsilon) \sim |\varepsilon|$ increases, with increasing disorder. With this notion we numerically estimate the crossover boundary between the WSM and the critical regime at finite energy [see Fig. 2(a)]. When $W = W_c$, the mean DOS displays a $|\varepsilon|$ -linear dependence over the entire energy range ($|\varepsilon| < 0.5$). For $W > W_c$, $|\varepsilon|$ -linear behavior of $\varrho(\varepsilon)$ ceases at finite energy, defining the boundary between the CDM and critical regime [see Fig. 2(a)].

Conclusions. To conclude, we show that WSM is stable against weak disorder, but undergoes a QPT and becomes a CDM at strong disorder. Across such a QPT the MDOS displays single-parameter scaling. The critical exponents (ν, z) appear to be independent of the number of Weyl nodes (N_W)

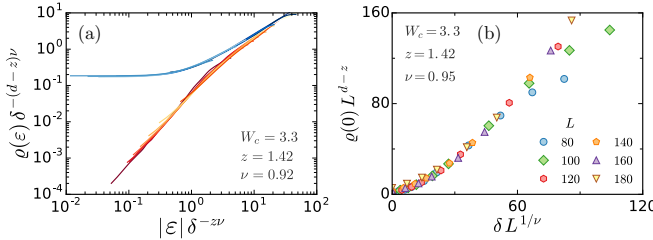


FIG. 5. (a) Single-parameter scaling of MDOS in WSM ($N_w = 1$) with $L = 220$. The top (bottom) branch corresponds to CDM (WSM). (b) Data collapse for $\rho(0, L)$ when $N_w = 1$. For large δ , deviations from single-parameter scaling stem from the Anderson transition at strong disorder.

(see Table I), since contribution from any *fermionic bubble* vanishes in the vanishing replica limit [28]. The extent of the critical regime at finite energy associated with such a QCP [see Fig. 2(a)] can also be measured from angle-resolved photoemission spectroscopy (ARPES) or scaling of specific heat ($C_v \sim T^{d/z}$) in various WSMs [7–16] and topological Dirac semimetals (two superimposed copies of WSMs), such as Cd_2As_3 [49] and Na_3Bi [50]. In contrast, the double WSM becomes CDM for weak (infinitesimally small in the thermodynamic limit) disorder. While in the metallic phase $C_v \sim T$, in WSM and double WSM specific heat scales as $C_v \sim T^3$ and T^2 , respectively [45]. Therefore, as a function of temperature, specific heat in double WSM should display a smooth crossover from T^2 to T dependence as the temperature

is gradually decreased [see Fig. 2(b)]. Generalization of the scaling analysis dictates that weak disorder is a *relevant* perturbation in *triple WSM* (monopole charges ± 3), since $[\Delta] = 1 - \frac{2}{n} = \frac{1}{3}$ for $n = 3$. Therefore, among various three-dimensional topological semimetals, only conventional WSM is stable against weak disorder [51].

Finally, we discuss the transport phenomena in disordered Weyl systems. In weakly disordered WSM ($W < W_c$), the optical conductivity (in collisionless regime) displays a smooth crossover from $\sigma_{jj}(\Omega) \sim \Omega$ to $\Omega^{1/z}$ dependence as frequency (Ω) is increased, closely following the phase diagram in Fig. 2(a) for $j = x, y, z$ [34]. In the strong disorder regime ($W > W_c$), $\sigma_{jj}(\Omega)$ becomes finite as $\Omega \rightarrow 0$. By contrast, in double and triple WSMs, $\sigma_{zz}(\Omega) \sim \Omega$, while $\sigma_{xx/yy}(\Omega) \sim \Omega^{1/n}$ at high frequency with $n = 2$ and 3 , respectively. However, as $\Omega \rightarrow 0$, σ_{jj} becomes finite in these two systems for arbitrary strengths of disorder and for any j . Scaling of dc conductivity (collision dominated) follows those for optical conductivity upon taking $\Omega \rightarrow T$. Thus, in the future one can probe the transport properties to establish the global phase diagram of disordered Weyl materials at finite frequency and temperature.

Acknowledgments. J.D.S. and B.R. were supported by the startup grant of J.D.S. from University of Maryland. We thank the visitor program of Max Planck Institute for Complex Systems, Dresden for hospitality during the final stage of the work. We are thankful to J. H. Bardarson, S. Das Sarma, P. Goswami, I. F. Herbut, K. Imura, V. Jurić, and J. Pixley for valuable discussions.

-
- [1] M. Z Hassan and C. L. Kane, *Rev. Mod. Phys.* **82**, 3045 (2010).
[2] X. L. Qi and S.-C. Zhang, *Rev. Mod. Phys.* **83**, 1057 (2011).
[3] B.-J. Yang and N. Nagaosa, *Nat. Commun.* **5**, 4898 (2014).
[4] T. Morimoto and A. Furusaki, *Phys. Rev. B* **89**, 235127 (2014).
[5] H. B. Nielsen and M. Ninomiya, *Nucl. Phys. B* **185**, 20 (1981); *Phys. Lett. B* **105**, 219 (1981).
[6] For review, see A. A. Burkov, *J. Phys.: Condens. Matter* **27**, 113201 (2015), and references therein.
[7] C. Zhang, Z. Yuan, S. Xu, Z. Lin, B. Tong, M. Z. Hasan, J. Wang, C. Zhang, and S. Jia, [arXiv:1502.00251](https://arxiv.org/abs/1502.00251).
[8] S.-Y. Xu, I. Belopolski, N. Alidoust, M. Neupane, C. Zhang, R. Sankar, S.-M. Huang, C.-C. Lee, G. Chang, B. Wang, G. Bian, H. Zheng, D. S. Sanchez, F. Chou, H. Lin, S. Jia, and M. Z. Hasan, *Science* **349**, 613 (2015).
[9] B. Q. Lv, H. M. Weng, B. B. Fu, X. P. Wang, H. Miao, J. Ma, P. Richard, X. C. Huang, L. X. Zhao, G. F. Chen, Z. Fang, X. Dai, T. Qian, and H. Ding, *Phys. Rev. X* **5**, 031013 (2015).
[10] S.-Y. Xu, N. Alidoust, I. Belopolski, C. Zhang, G. Bian, T.-R. Chang, H. Zheng, V. Strokov, D. S. Sanchez, G. Chang, Z. Yuan, D. Mou, Y. Wu, L. Huang, C.-C. Lee, S.-M. Huang, B. Wang, A. Bansil, H.-T. Jeng, T. Neupert, A. Kaminski, H. Lin, S. Jia, and M. Z. Hasan, *Nat. Phys.* **11**, 748 (2015).
[11] N. Xu, H. M. Weng, B. Q. Lv, C. Matt, J. Park, F. Bisti, V. N. Strocov, D. Gawryluk, E. Pomjakushina, K. Conder, N. C. Plumb, M. Radovic, G. Aut, O. V. Yazyev, Z. Fang, X. Dai, G. Aeppli, T. Qian, J. Mesot, H. Ding, and M. Shi, *Nat. Commun.* **7**, 11006 (2016).
[12] C. Shekhar, A. K. Nayak, Y. Sun, M. Schmidt, M. Nicklas, I. Leermakers, U. Zeitler, Z. Liu, Y. Chen, W. Schnelle, J. Grin, C. Felser, and B. Yan, *Nat. Phys.* **11**, 645 (2015).
[13] Z. Wang, Y. Zheng, Z. Shen, Y. Zhou, X. Yang, Y. Li, C. Feng, and Z.-A. Xu, *Phys. Rev. B* **93**, 121112 (2016).
[14] G. Chang, S.-Y. Xu, D. S. Sanchez, S.-M. Huang, C.-C. Lee, T.-R. Chang, H. Zheng, G. Bian, I. Belopolski, N. Alidoust, H.-T. Jeng, A. Bansil, H. Lin, and M. Z. Hasan, [arXiv:1512.08781](https://arxiv.org/abs/1512.08781).
[15] S. Borisenko, D. Evtushinsky, Q. Gibson, A. Yaresko, T. Kim, M. N. Ali, B. Buechner, M. Hoesch, and R. J. Cava, [arXiv:1507.04847](https://arxiv.org/abs/1507.04847).
[16] J. Y. Liu, J. Hu, Q. Zhang, D. Graf, H. B. Cao, S. M. A. Radmanesh, D. J. Adams, Y. L. Zhu, G. F. Cheng, X. Liu, W. A. Phelan, J. Wei, D. A. Tennant, J. F. DiTusa, I. Chiorescu, L. Spinu, and Z. Q. Mao, [arXiv:1507.07978](https://arxiv.org/abs/1507.07978).
[17] X. Wan, A. M. Turner, A. Vishwanath, and S. Y. Savrasov, *Phys. Rev. B* **83**, 205101 (2011).
[18] P. Goswami, B. Roy, and S. Das Sarma, [arXiv:1603.02273](https://arxiv.org/abs/1603.02273).
[19] A. A. Burkov and L. Balents, *Phys. Rev. Lett.* **107**, 127205 (2011).
[20] A. A. Zyuzin, S. Wu, and A. A. Burkov, *Phys. Rev. B* **85**, 165110 (2012).

- [21] C. X. Liu, P. Ye, and X. L. Qi, *Phys. Rev. B* **87**, 235306 (2013).
- [22] C. Fang, M. J. Gilbert, X. Dai, and B. A. Bernevig, *Phys. Rev. Lett.* **108**, 266802 (2012).
- [23] S.-M. Huang, S.-Y. Xu, I. Belopolski, C.-C. Lee, G. Chang, B. Wang, N. Alidoust, M. Neupane, H. Zheng, D. Sanchez, A. Bansil, G. Bian, H. Lin, and M. Z. Hasan, *Proc. Natl. Acad. Sci. USA* **113**, 1180 (2016).
- [24] E. Fradkin, *Phys. Rev. B* **33**, 3263 (1986).
- [25] R. Shindou and S. Murakami, *Phys. Rev. B* **79**, 045321 (2009).
- [26] P. Goswami and S. Chakravarty, *Phys. Rev. Lett.* **107**, 196803 (2011).
- [27] Y. Ominato and M. Koshino, *Phys. Rev. B* **89**, 054202 (2014).
- [28] B. Roy and S. Das Sarma, *Phys. Rev. B* **90**, 241112(R) (2014); **93**, 119911(E) (2016).
- [29] S. V. Syzranov, L. Radzihovsky, and V. Gurarie, *Phys. Rev. Lett.* **114**, 166601 (2015); S. V. Syzranov, V. Gurarie, and L. Radzihovsky, *Phys. Rev. B* **91**, 035133 (2015).
- [30] R. Nandkishore, D. A. Huse, and S. L. Sondhi, *Phys. Rev. B* **89**, 245110 (2014).
- [31] Z. Huang, D. P. Arovas, and A. V. Balatsky, *New J. Phys.* **15**, 123019 (2013).
- [32] B. Skinner, *Phys. Rev. B* **90**, 060202 (2014).
- [33] A. Altland and D. Bagrets, *Phys. Rev. Lett.* **114**, 257201 (2015).
- [34] B. Roy, V. Juričić, and S. Das Sarma, *arXiv:1603.00017*.
- [35] K. Kobayashi, T. Ohtsuki, and K.-I. Imura, *Phys. Rev. Lett.* **110**, 236803 (2013).
- [36] K. Kobayashi, T. Ohtsuki, K.-I. Imura, and I. F. Herbut, *Phys. Rev. Lett.* **112**, 016402 (2014).
- [37] B. Sbierski, G. Pohl, E. J. Bergholtz, and P. W. Brouwer, *Phys. Rev. Lett.* **113**, 026602 (2014).
- [38] J. H. Pixley, P. Goswami, and S. Das Sarma, *Phys. Rev. Lett.* **115**, 076601 (2015).
- [39] B. Sbierski, E. J. Bergholtz, and P. W. Brouwer, *Phys. Rev. B* **92**, 115145 (2015).
- [40] J. H. Pixley, P. Goswami, and S. Das Sarma, *Phys. Rev. B* **93**, 085103 (2016).
- [41] C.-Z. Chen, J. Song, H. Jiang, Q.-F. Sun, Z. Wang, and X. C. Xie, *Phys. Rev. Lett.* **115**, 246603 (2015).
- [42] S. Liu, T. Ohtsuki, and R. Shindou, *Phys. Rev. Lett.* **116**, 066401 (2016).
- [43] H. Shapourian and T. L. Hughes, *Phys. Rev. B* **93**, 075108 (2016).
- [44] J. H. Pixley, D. A. Huse, and S. Das Sarma, *arXiv:1602.02742*.
- [45] See Supplemental Material at <http://link.aps.org/supplemental/10.1103/PhysRevB.93.201302> for a renormalization group analysis and numerical results for double WSM, numerical results for WSM with $N_W = 2, 4$, details of the tight-binding model, the numerical method, and scaling of specific heat in dirty double WSM.
- [46] A. Weiße, G. Wellein, A. Alverman, and H. Feshke, *Rev. Mod. Phys.* **78**, 275 (2006).
- [47] S. Sachdev, *Quantum Phase Transitions*, 2nd ed. (Cambridge University Press, Cambridge, UK, 2007).
- [48] I. F. Herbut, *A Modern Approach to Critical Phenomena* (Cambridge University Press, Cambridge, UK, 2007).
- [49] S. Borisenko, Q. Gibson, D. Evtushinsky, V. Zabolotnyy, B. Büchner, and R. J. Cava, *Phys. Rev. Lett.* **113**, 027603 (2014).
- [50] Z. K. Liu, B. Zhou, Y. Zhang, Z. J. Wang, H. M. Weng, D. Prabhakaran, S.-K. Mo, Z. X. Shen, Z. Fang, X. Dai, Z. Hussain, and Y. L. Chen, *Science* **343**, 864 (2014).
- [51] P. Goswami and A. H. Nevidomskyy, *Phys. Rev. B* **92**, 214504 (2015); P. Goswami and L. Balicas, *arXiv:1312.3632*.